FULL RESEARCH ARTICLE

Blended structural optimization for wire-and-arc additively manufactured beams

Vittoria Laghi[1] · Michele Palermo[1] · Matteo Bruggi[2] · Giada Gasparini[1] · Tomaso Trombetti[1]

© The Author(s) 2022

Abstract
Current manufacturing techniques in the construction sector are slow, expensive and constrained in terms of architectural shapes. In other manufacturing sectors (such as automotive and aerospace) the use of automated construction systems significantly improved the safety, speed, quality and complexity of products. To realize real-scale structural elements for construction applications without ideally any geometrical constraints either in size or shape, the most suitable manufacturing solution for metallic elements is a directed energy deposition (DED) process referred to as wire-and-arc additive manufacturing (WAAM). The main advantage of WAAM relies on the possibility to create new shapes and forms following the breakthrough design tools for modern architecture as algorithm-aided design. At the same time, the printed part ensures high structural performances with reduced material use with respect to the conventional solution. The study presents a new approach called "blended" structural optimization, which blends topology optimization with basic principles of structural design and manufacturing constraints proper of WAAM technology, towards the realization of new efficient structural elements. The approach is applied to the case study of a I-type stainless steel beam on a multi-storey frame building. The approach could pave the way towards an efficient use of WAAM process to produce a new generation of structurally optimized elements for construction, with a more conscious use of the optimization tools and an efficient application of metal 3D printing.

Keywords Additive manufacturing · Wire-and-arc · Orthotropic model · Topology optimization · Numerical simulations

1 Introduction

The digitalization of the construction sector has the potential to produce more efficient structures, reduce material waste and increase work safety [1–3]. In particular, the application of additive manufacturing (AM) has proved to support the Circular Economy by (1) offering new raw material options, (2) increasing the efficiency of the fabricated designs thus reducing the in-production waste and (3) simplifying the resource recapture, hence supporting composting and recycling [4]. Among different AM processes, wire-and-arc additive manufacturing (WAAM) appears the most suitable for large metal structural elements with 50% reduction in

CO2 emissions [5]. Moreover, breakthrough design tools for modern architecture as algorithm-aided design (AAD) could be used to increase the structural efficiency and thus further reduce the environmental impact of the construction industry. However, high-skilled professionals are needed to fully apply automation in construction [6]. Recent applications of WAAM for large-scale structures exploited two different deposition strategies: (1) a "continuous" strategy, i.e., layer-by-layer deposition, suitable for planar and shell elements [7, 8] and (2) a "dot-by-dot" strategy to realize lattice and diagrid structures [9]. With reference to WAAM elements, specific considerations must be made on: (1) the inherent surface roughness, which could influence the mechanical properties [10, 11], (2) the marked mechanical anisotropy due to the specific microstructure [12, 13], (3) the influence of process parameters in both geometrical and mechanical response [14]. Hence, specific knowledge in advanced manufacturing technology should be combined with structural design competences to efficiently fabricate high-strength WAAM elements. Intensive effort in this sense was made by the Dutch company MX3D in collaboration

✉ Vittoria Laghi
vittoria.laghi2@unibo.it

[1] DICAM-Department of Civil, Chemical, Environmental and Materials Engineering, University of Bologna, Bologna, Italy

[2] Department of Civil and Environmental Engineering, Politecnico di Milano, Milan, Italy

Springer

with the research team from Imperial College of London to design and fabricate the world's first 3D printed steel footbridge (see, e.g., [7]). Recently, an automated end-to-end framework for the generation of high-performance AM structures was implemented to integrate AM techniques into the construction of optimized members [15].

The use in recent decades of computational design technologies resulted in the development of new structures with formal freedom and ideally infinite complexity, often designed to aim for structural efficiency. Nonetheless, current building production still does not allow for such freedom. Hence, the application of computational design tools for free-form design is often limited to few explorations in pioneering architectural applications. Generally speaking, the concept of structural optimization aims at acquiring new structural shapes in place of initial domain through an algorithmic process. The common approach is to make use of topology optimization, a powerful design tool to sketch lightweight structural components [16]. In detail, topology optimization defines the material distribution making an optimal component within a design domain, based on the minimization of an objective function and a given set of constraints. Thus, it is a useful tool for designing new lightweight structural elements [17, 18]. With the advent of AM processes, the scientific community has paid lot of effort towards their implementation in topology optimization tools to leverage the full potential of their combined use [19, 20]. However, specific geometrical and mechanical features different for each set of printing parameters need to be properly accounted.

The present study aims at providing new insights into an innovative overarching computational design approach guiding the designer from an initial conceptual design to a final optimized design integrating conceptual design with structural optimization accounting for manufacturing constraints approach, here referred to as "blended structural optimization". The term "blended" derives from the idea of blending the theoretical optimization tools with basic principles and solutions coming from structural engineering knowledge. Section 2 presents the WAAM approach and the design issues proper of this printing process. Section 3 illustrates different structural design approaches, while in Sect. 4 the blended structural design approach is presented and applied to a case study (Sect. 5).

2 Wire-and-arc additive manufacturing (WAAM)

2.1 WAAM process

This study refers to wire-and-arc additive manufacturing (WAAM) process to realize new-generation optimized structural elements. In particular, the authors have been studying WAAM-produced 308LSi stainless steel plates from the microstructural, geometrical and mechanical point of view [10, 13, 21]. The plates were printed with Gas Metal Arc Welding (GMAW), pulse arc metal transfer and using the continuous printing strategy, consisting in the deposition of successive layers of welded metal one over the other to create planar or extruded elements with constant thickness. The fundamental process parameters for WAAM are: (1) the current and its voltage, (2) the wire diameter, (3) the wire-feed rate, (4) the welding speed and (5) the vertical printed layer height. The combination of such controlling parameters highly affects the printing quality (geometrical precision and surface roughness) as well as the material mechanical properties [14].

The high printing velocity required to fabricate large-scale elements for structural applications induce some non-negligible geometrical irregularities of the printed outcomes [10, 22–24]. Hence, additional considerations on the identification of the best printing strategy and set of process parameters is crucial to reduce these imperfections [25].

2.2 Design issues and possibilities

WAAM-produced planar elements are characterized by specific inherent geometrical irregularities, proper of WAAM layer-by-layer printing process, and specific material behavior, typically governed by a marked anisotropy. Both aspects need to be properly taken into account and fully characterized for structural design of WAAM-produced elements, as they are both sources of uncertainties which influence the structural response of the designed as-printed elements.

The first peculiar aspect when dealing with structural members realized with WAAM process is related to the geometrical irregularities of the printed outcome. As far as the continuous printing strategy is concerned, the main issue related to the layer-by-layer deposition is the surface roughness which also causes variation in thickness of as-built specimens [10]. From planar to tubular geometries, additional irregularities in terms of lack of straightness and out-of-roundness also arise [26]. Therefore, for ready-to-use elements and future applications of on-site metal 3D printing, detailed studies on the geometrical irregularities of WAAM-produced structural elements have been carried out [10].

In addition, the manufacturing process is proven to influence the orientation of the microstructure, which affects the mechanical behavior of the printed parts [22, 27–31]. Hence, the mechanical response should be investigated with reference to specimens having different orientation with respect to the deposition layers. Figure 1 qualitatively depicts the main directions of a WAAM-produced plate, e.g., the one along the deposited layer (longitudinal direction) and the
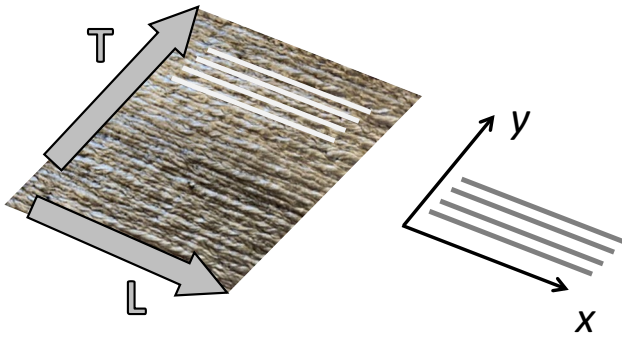
Fig. 1 Graphical representation of the coordinate systems adopted to describe the orthotropic material model for WAAM plates

one perpendicular to it (transversal direction). The general reference system describes the orientation of the printed layers, while the symmetry axes of the orthotropic medium are denoted as L (longitudinal direction) and T (transversal direction). Previous studies revealed a specific anisotropic relationship between the relative printing orientation and the mechanical response of WAAM-produced stainless steel plates, then modelled as an orthotropic material (as explained in the next section) [12, 32].

2.3 WAAM orthotropic elastic material model

WAAM stainless steel material is a layered material. This suggests the adoption of an orthotropic material model, whose symmetry axes x and y are the main deposition directions and the orthogonal one (longitudinal and transversal direction, L and T, respectively). As such, previous research

has been carried out to calibrate an orthotropic plane stress material model for WAAM stainless steel, validated through experimental tests [12, 32].

The analytical procedure that follows is fully reported in [12]. The stress–strain model of WAAM stainless steel is written in terms of the compliance matrix C:

$$C = \begin{bmatrix} 1/E_x & -v_{xy}/E_y & 0 \\ -v_{yx}/E_x & 1/E_y & 0 \\ 0 & 0 & 1/G_{xy} \end{bmatrix} \tag{1}$$

E_x and E_y are the Young's moduli along x and y, respectively, v_{xy}, and v_{yx} are the Poisson's ratios, and G_{xy} is the shear modulus. For WAAM plates the two principal directions (x,y) correspond to the main relative direction with respect to the printing layer (e.g., longitudinal direction L and transversal direction T). Hence, E_x and E_y are assumed as average values from experiments (see, e.g., [12]). Accordingly, the values of Poisson's ratios are obtained from the minimization problem based on the experimental data as:

$$\begin{cases} v_{xy} = \dfrac{E_x}{E_x + E_y} \cdot (v_{LT} + v_{TL}) \\ v_{yx} = \dfrac{E_y}{E_x + E_y} \cdot (v_{LT} + v_{TL}) \end{cases} \tag{2}$$

The terms v_{LT} and v_{TL} refer to the Poisson's ratios as evaluated from experiments. Figure 2 shows the normalized polar diagrams (with respect to the conventional 304L stainless steel from ASM Handbook [33]) of the Young's modulus and shear modulus (red continuous lines), as computed through transformation of the compliance matrix of Eq. 1, see, e.g., [12]. The orientation α is measured from x
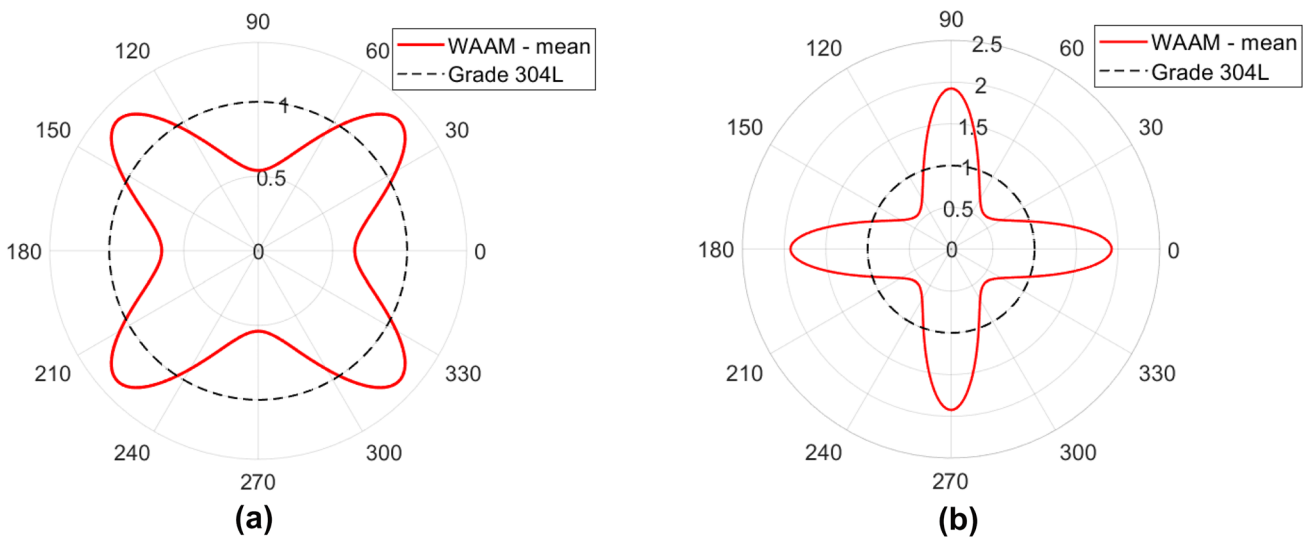

Fig. 2 Normalized polar diagrams: **a** Young's modulus and **b** shear modulus of WAAM-produced stainless steel and of Grade 304 stainless steel depending on the orientation of the reference system with respect to x. Adapted from [12]

(i.e., $\alpha = 0°$ corresponds to L direction on the real printed material, while $\alpha = 90°$ corresponds to T direction on the real printed material).

Concerning Young's modulus (Fig. 2a), the minimum values, as expected, are for $\alpha = \pm 90°$ and $\pm 180°$, along the transversal (T) direction of the WAAM printed plate, while the maximum values are found at around $\pm 45°$ and $\pm 135°$. As far as shear modulus is concerned (Fig. 2b), maximum values are registered for $\alpha = \pm 90°$ and $\pm 180°$, with values on average twice the one commonly adopted for 304L steel. Minimum values are, instead, quite below (almost halved) the standard value considered for 304L steel, at $\alpha = \pm 45°$ and $\alpha = \pm 135°$. Clearly the values reported in the diagrams of Fig. 2 are related to specific WAAM process. Nevertheless, the same procedure can be applied to any WAAM process.

The calibration of an orthotropic model for WAAM stainless steel would allow to draw unexplored design possibilities in structural design, in terms of new design strategies to exploit the different structural response based on the printing direction.

3 Structural design approaches for WAAM

3.1 Conventional design adapted to WAAM

The design approach most widely adopted in international standard building codes, including Eurocodes, is the so-called design value method, also referred to as semi-probabilistic method [34, 35], as first introduced in ISO 2394: "General principles on reliability for structures" [36].

This method is based on the assumption that no limit state is exceeded when the design values of all basic variables are used in the models of structural resistance R and action effect E. Thus, if the design values E_d and R_d are determined considering the design values of all basic variables, then a structure is considered reliable if the following inequality holds:

$$E_d < R_d \tag{3}$$

The action effect depends on the loads and actions applied, while the structural resistance depends on the material properties. Both of them also depend on the geometrical properties. Generally speaking, all these quantities are taken as random variables whose uncertainties depend also, in addition to the inherent uncertainties of the individual basic variables, on the model uncertainties. Clearly, for design purposes their design values should be considered.

With reference to traditional structures, the material properties (as well as the actions) are taken as random variables, whose distribution is evaluated with statistical analysis. On the other hand, the geometrical properties are typically considered as deterministic values given that their variability are generally negligible when considering traditional manufacturing processes. On the contrary, when dealing with AM process, there could be the need to also take into account for the inherent geometrical variabilities associated to the printing process. The structural models of typical frame structures adopted to evaluate the structural response are usually assembled considering beam elements according to the De Saint Venant's theory and assuming a linear elastic material behaviour.

When dealing with WAAM elements, such approach should be based on the use of effective properties, in terms of effective stresses and strains accounting for volume-equivalent uniform geometries corresponding to uniform distribution of stresses and strains along the element (see, e.g., [10]) and various sources of uncertainties including those related to the inherent geometrical variabilities. Therefore, for structural design purposes, ad-hoc design values and partial safety factors of the key effective mechanical parameters should be properly calibrated, based on the specific printing process highly affecting both the anisotropic nature of the printed material and the variability in the response of the printed part (see, e.g., [37]).

3.2 Design assisted by advanced modelling and non-linear analysis

Within the design workflow of AM parts and components, advanced numerical models should be adopted to account for the specific issues related to the printing process, such as the levels of anisotropy, the geometrical imperfections or the residual stresses.

As such, a new design approach referred to as "design by advanced analysis" has been developed to exploit the full advantages and characteristics of AM technology. The basic principle lies within the concept of the so-called "digital twin", i.e., the mirroring of a physical object created in a virtual environment by simulation-based engineering [38]. These advanced simulation tools would allow to: (1) accurately model all geometrical imperfections of the manufactured part; (2) consider the real material behavior (i.e., orthotropic material model); (3) simulate different loading and boundary conditions to which the part could be subjected. Recent application of such pioneering research was developed by a team from Alan Turin Institute in collaboration with the Imperial College of London and Autodesk to reproduce a digital twin of the MX3D Bridge, the world's first metal 3D printed footbridge [7]. Nevertheless, such advanced simulation tools require high computational skills beyond the capabilities of professional structural engineers [6].

3.3 Computational design approach

Recently, a paradigm shift has occurred in the structural design workflow thanks to the computational design concept, that fully entails the use of computation for the exploration of structural solutions and the development of novel design ideas.

Within computational design framework, different approaches have been proposed so far. Cascone et al. recently proposed a structural grammar approach for the generative design of diagrid-like structures [39]. A similar concept has been adopted to realize a WAAM diagrid column [9]. Generative design has also been used by Wang et al. in an integrated method to create joints for tree-like columns to be realized in AM [40]. Alternatively, topology optimization algorithms have been implemented to consider the features proper of AM process [19, 41]. With reference to the latter, Kanyilmaz et al. recently proposed innovative steel tubular joints designed by making use of topology optimization and metal AM techniques by mimicking features present in nature [42]. Recently, a new formulation to implement manufacturing constraints and printing orientation in topology optimization algorithms has been proposed to realize a new generation of WAAM-produced planar elements. In detail, a displacement-constrained minimum weight formulation for WAAM stainless steel plates accounting for the orthotropic material model has been developed. Numerical simulations revealed that the build orientation remarkably affects the shape and stiffness of the optimal layouts in case of single-plate specimens [43]. The same formulation has been extended to propose optimal design of WAAM-produced stainless steel I-beams [44].

4 The "blended" structural optimization approach

With the aim of integrating the capabilities of optimization procedures in terms of new structural shapes with the current limitations of WAAM technology (i.e., manufacturing constraints, printing precision and material properties) together with the robustness and reliability of structural design verifications, a so-called blended structural optimization approach is here proposed. Indeed, the approach is intended to "blend" a stiffness-based topology optimization approach (suitably tailored for WAAM stainless steel, see, e.g., [43]) with basic principles of structural design in terms of conceptual design and structural solutions to conceive an initial design, together with concepts of robustness and reliability to guide the designer from the purely mathematically optimized solutions towards the final design. In fact, the optimized designs need to comply with the manufacturing constraints proper of WAAM process,

and then to be structurally verified through numerical simulations using an iterative process towards the final design. This could be achieved by endowing the proposed optimization approach with multiple sets of constraints involving non-linearities, at the cost of increased complexity and computational time. A blended structural optimization approach may be conveniently used to investigate effective solutions in an efficient way. The fundamental aspects of the blended design approach, namely, the basic principles, the manufacturing constraints, the algorithms for topology optimization, the numerical simulations to verify the structural performances, are represented in the schematic of Fig. 3.

Figure 4 presents the conceptual flowchart of the blended structural optimization approach through various steps. (1) First, an initial design is set based on solutions coming from the past and from basic principles of structural engineering. (2) From that, the target performances are formulated in terms of structural behavior (serviceability and ultimate limit states), economic and functional requirements (costs, aesthetics, …). (3) The definition of the modelling criteria and assumptions is set in terms of: (i) domain definition, (ii) material behavior and (iii) manufacturing constraints, such as printing angles, allowable thickness range, etc. (4) Based on the predicted application, the boundary conditions are set in terms of support definition and load cases. (5) The optimization problem is then formulated based on a subset of the data provided in (3, 4) to achieve the target objectives (2). This process is included in an iterative procedure in which the optimized design is first selected through a topology optimization algorithm seeking for lightweight design with prescribed stiffness, then verified in terms of its structural performances through numerical simulations. (6) Lastly, the final design is selected among the optimized designs that comply with the requested structural performances (2).
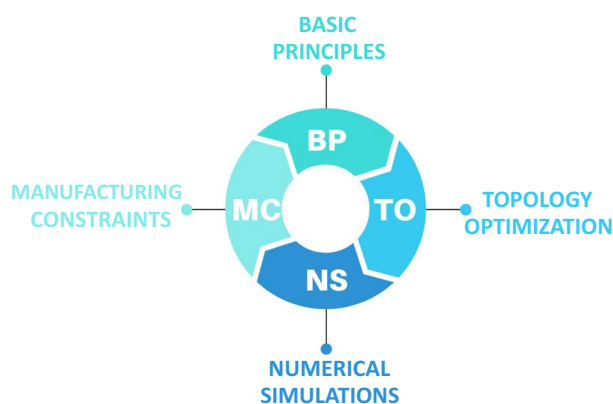

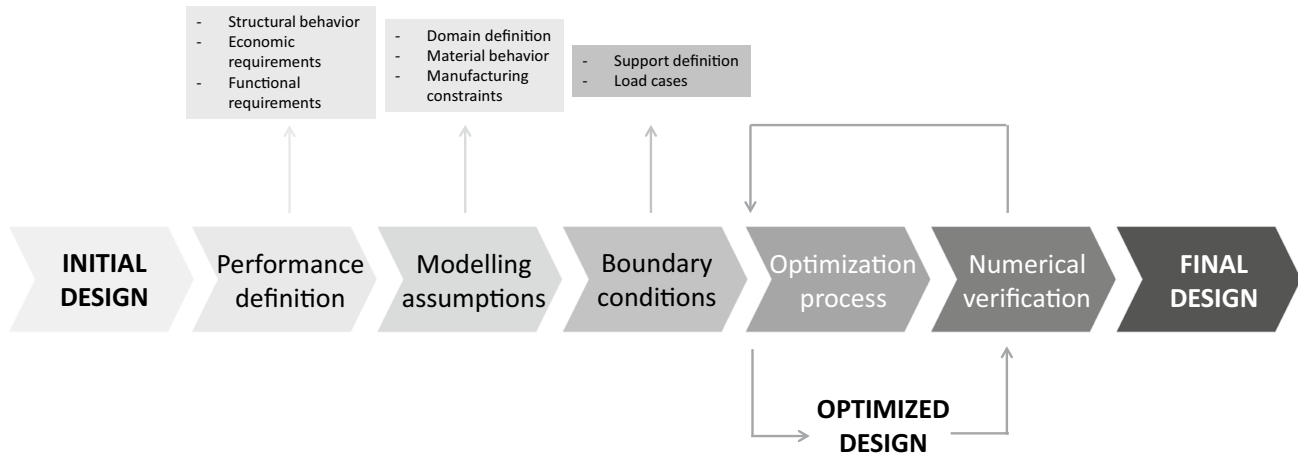**Fig. 3** Fundamental aspects of the blended structural optimization approach

Fig. 4 Conceptual flowchart of the blended structural optimization approach

Fig. 5 3D graphical representation of optimized I-type beams for a multi-storey steel frame building

5 Case study

In the present section the blended structural optimization approach is applied to the case study of a stainless steel beam of 4.5 m length to be inserted in a multi-storey frame building (Fig. 5).

5.1 Initial design, target performances, material properties and boundary conditions

First, the initial design is set as a European I-type profile IPE300 considering the usual height-to-length ratio rules commonly adopted by practitioners in the preliminary design phase. The beam is intended to be manufactured in WAAM stainless steel, considering the material properties and orthotropic nature proper of the printed plates as presented in Sect. 2.3.

Given that the beam is going to be placed in a braced steel frame structure, the typical boundary conditions are hinge-type beam–column connections. Hence, two different sets of supports can be considered: (1) a doubly hinged beam and (2) a hinge–roller beam to account for the possible lateral displacement of the columns. By looking at the flow of the principal stresses of a beam under a uniformly distributed load with these two support conditions (as schematically represented in Fig. 6) some considerations can be made. It is clear that the presence of two hinges (Fig. 6a) determines the formation of compressed arched struts (in blue) going from the extrados directly to the two supports, in combination of few central straight compressed struts sustained by a reversed tie (in red) subjected to tension. The hinge–roller condition (Fig. 6b) requires the presence of a system of trusses and ties forming a net characterized by a straight tie located at the intrados which supports the compressed arched struts coming from the extrados, as well as a series of curved ties going from the two sides of the extrados to the center of the intrados. The latter solution is more costly (in terms of amount of material) but also more robust, as it is less sensitive to possible relative lateral displacements between the two supports. Indeed, in real constructions it is unavoidable to have slight relative displacements in the supports, which can behave in between the two limit cases. Hence, the hinge–roller boundary condition is set for the procedure.
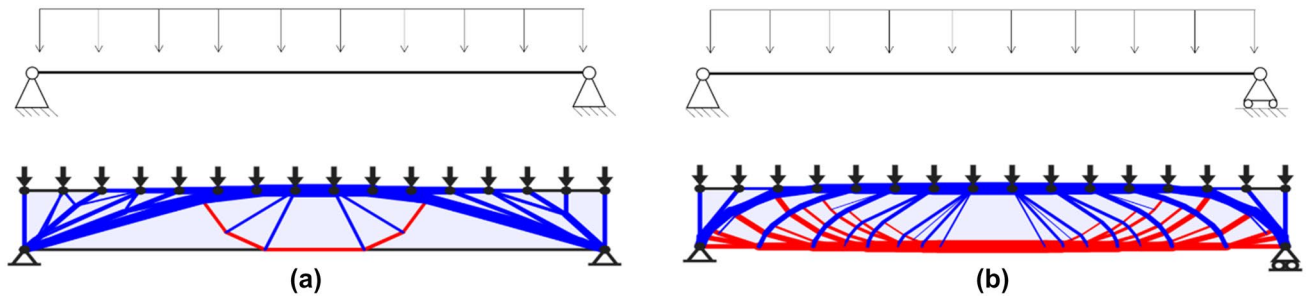
Fig. 6 Double-hinge (**a**) vs. hinge–roller (**b**) boundary supports (stress lines adapted from [45])

5.2 Load cases and optimal design

Topology optimization by distribution of WAAM orthotropic material is used to define the optimal shape of the I-beam under displacement constraints.

At first a discrete design domain is prescribed: four-node plane-stress elements are used to model the rectangular web plate, whereas trusses are used to account for the two web plates. In both cases, the printing orientation is accounted by prescribing a suitable constitutive law. The optimization problem is set, whose variables are the "density" of the material in each one of the plane elements sketching the web (a value between 0 and 1 scales the stiffness matrix of the relevant finite element according to standard interpolations, see [37]), and the width of the cross-section in each truss sketching the flanges (see [38]). The objective function is the overall weight, whereas constraints are enforced to the vertical displacement of the loaded points. The problem is solved by means of mathematical programming. The solution consists of maps of distribution of material "density" in the web and thickness in the flanges, both providing the optimal shape of an I-beam fulfilling the enforced set of displacement limits. In general, multiple load cases are considered, meaning that the achieved design is feasible with respect to the enforced displacement limits for all the prescribed load cases. The computational cost of the procedure is tied to the number of constraints. Besides the efficient implementation given in [37], in view of the efficiency requested to the herein proposed blended optimization approach, the controlled displacements in case of distributed loads are monitored at the mid-span, along with an average deflection measured over the beam length.

As far as the loading cases are concerned, different configurations are here envisaged, such as point-load cases, fully distributed cases and even asymmetric loads (Fig. 7) to investigate the sensitivity of the optimized solutions to the applied loads. Hence, for the optimization process, the following load cases are considered for the variable load
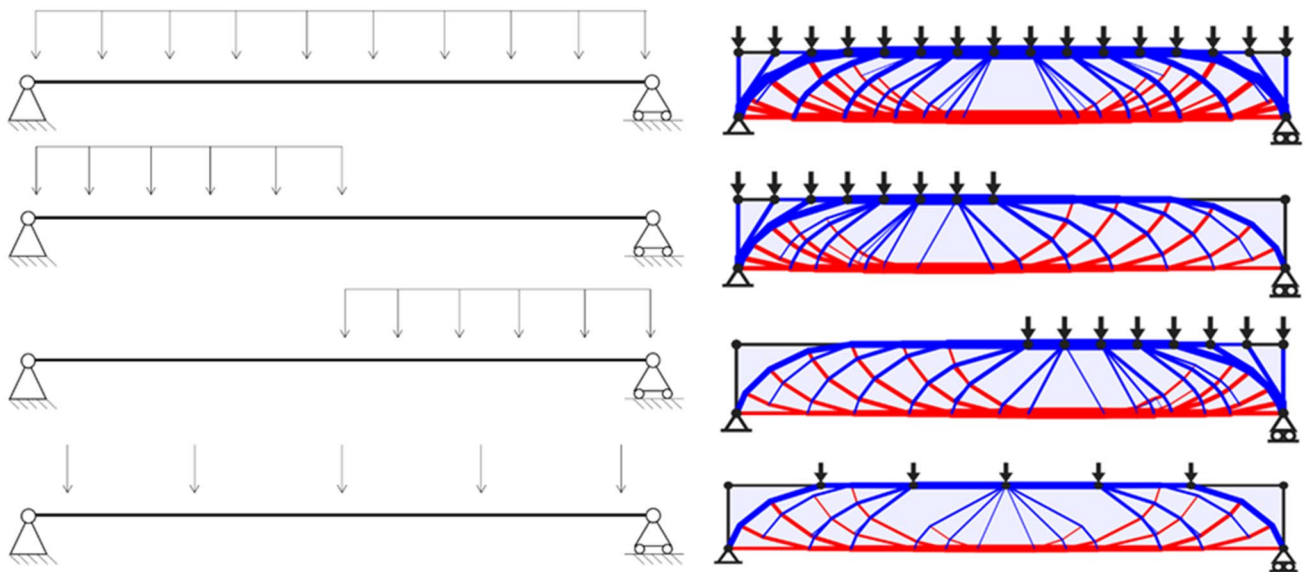

Fig. 7 Variable load cases investigated (adapted from [45])

condition (q_v): (1) fully distributed load, (2) asymmetric load distributed on the left-hand side and on the right-hand side, respectively, (3) 5-point load. All the load cases are associated to a constant permanent distributed load (q_p) assumed to be equal to 22.5 kN/m, resulting from the typical dead loads (self-weight of the structural elements plus non-structural elements) of a regular multi-storey steel frame structure. The variable load for all the investigated cases corresponds to an action equal to 27.5 kN/m, typical of a building subjected to crowding load (e.g., museums, libraries, etc.), so that the global distributed (sum of permanent and variable) load to the beam results equal to 50 kN/m (for all considered cases).

The optimization process is performed through a tailored topology optimization algorithm (as presented in [44]). The maximum allowable vertical displacement at the loaded points is set equal to $L/250$, where L is the length of the beam (corresponding to the bay width of a steel frame structure), in accordance with the European standard regulations for steel frames [46].

Figure 8 reports the optimized designs for four main printing orientations of the web (e.g., at 0°, 45°, 90° and 135° with respect to the deposition layers), considering the orthotropic material model for WAAM stainless steel (see Sect. 2.3). The flanges are designed considering a fixed printing orientation of 45° (which corresponds from the orthotropic model from Fig. 2 to the direction of maximum stiffness). Details on the topology optimization procedure for the web and the shape optimization procedure for the flanges can be found in [44], with special regard to the efficient implementation for gradient-based minimization algorithm.

From the basic principles of structural design, it is preferred to design load-bearing structural elements able to sustain different load cases, rather than being optimized for one specific case (which might be difficult to realize in real-case scenarios). Hence, instead of using standard volume-constrained minimum energy procedures, the optimization process is performed considering simultaneously all four variable load conditions previously selected within a displacement-constrained framework. As such, the final optimized design is able to guarantee the prescribed structural performances (i.e., maximum allowable displacement) for all the four cases considered. The optimized design is found as the one printed with 0° printing orientation, having 44.7% volume reduction from the initial design.

5.3 Structural verification through non-linear finite element analysis and final design

The final step of the blended structural optimization approach is the structural verification through numerical
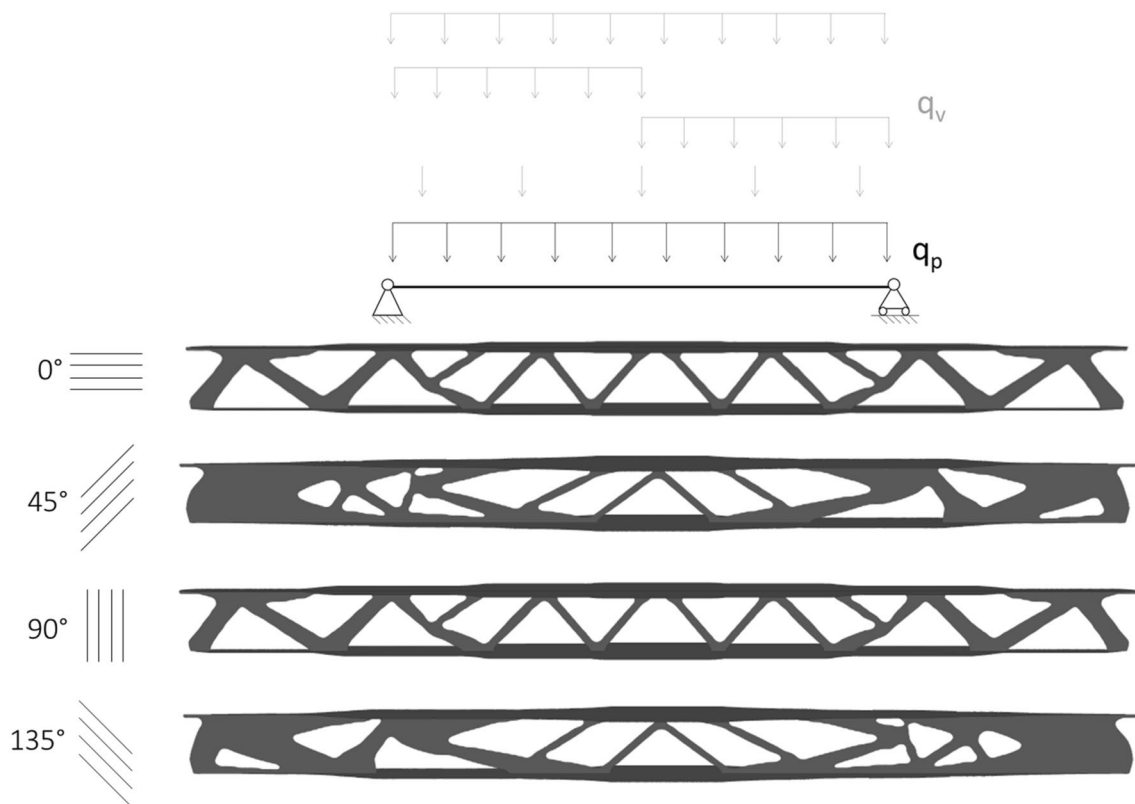
Fig. 8 Results of the optimization process

simulations. The optimized design is analyzed using the Finite Element Method (FEM) software Abaqus [47]. The imported geometry is meshed with a 6-node triangular thin shell mesh type. Regarding the material model, a simplified Ramberg–Osgood (RO) [48] with Rasmussen [49] material model is used for the material constitutive model. In particular, the model was calibrated from the average values obtained from experiments on WAAM stainless steel plates considering each of the three printing direction as a simplified isotropic material model [12]. The material constitutive model associated to the web part corresponds to the constitutive model calibrated from 0° printing orientation, considering an isotropic material model. The same procedure applies for the flanges, in which the constitutive model corresponds to the one calibrated from 45° printing orientation. Figure 9 reports the stress–strain curves for both printing orientations (0° and 45°) in terms of mean engineering values, e.g., calibrated from experimental results, and the corresponding true values, adopted for the analysis. For more accurate analyses, a calibrated orthotropic material model for both elastic and post-yielding behavior should be implemented (see, e.g., [32]).
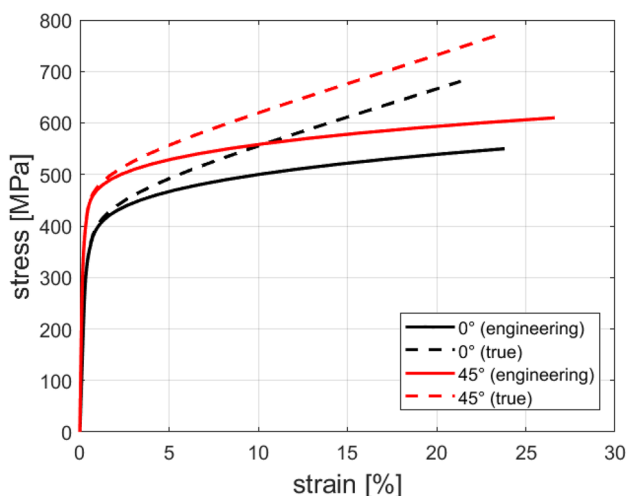
The beam is simulated with a hinge–roller support condition and uniformly distributed load applied on the upper flange equal to 50 kN/m (corresponding to the sum of permanent and variable loads). From the results, the maximum displacement that the optimized beam could sustain is equal to 7.92 mm at the mid-span, well below the serviceability limit state corresponding to $L/250$ (equal to 18 mm, see Fig. 10). As expected, this is not the worst case the I-beam has been optimized for. Even though the WAAM alloy exhibits a remarkable anisotropy in terms of elastic modulus, experimental tests showed that the yielding stress is less affected by the tested orientation. Hence, at least in a preliminary investigation, the Von Mises stress measure can be adopted for a preliminary assessment of the strength of the achieved design. The stress map (Fig. 11) confirms that the maximum stresses are located at the supports and are below 400 MPa, corresponding to the yielding stress for WAAM stainless steel at 45° printing direction (see, e.g., [13]). Not significant stress concentration arises, except
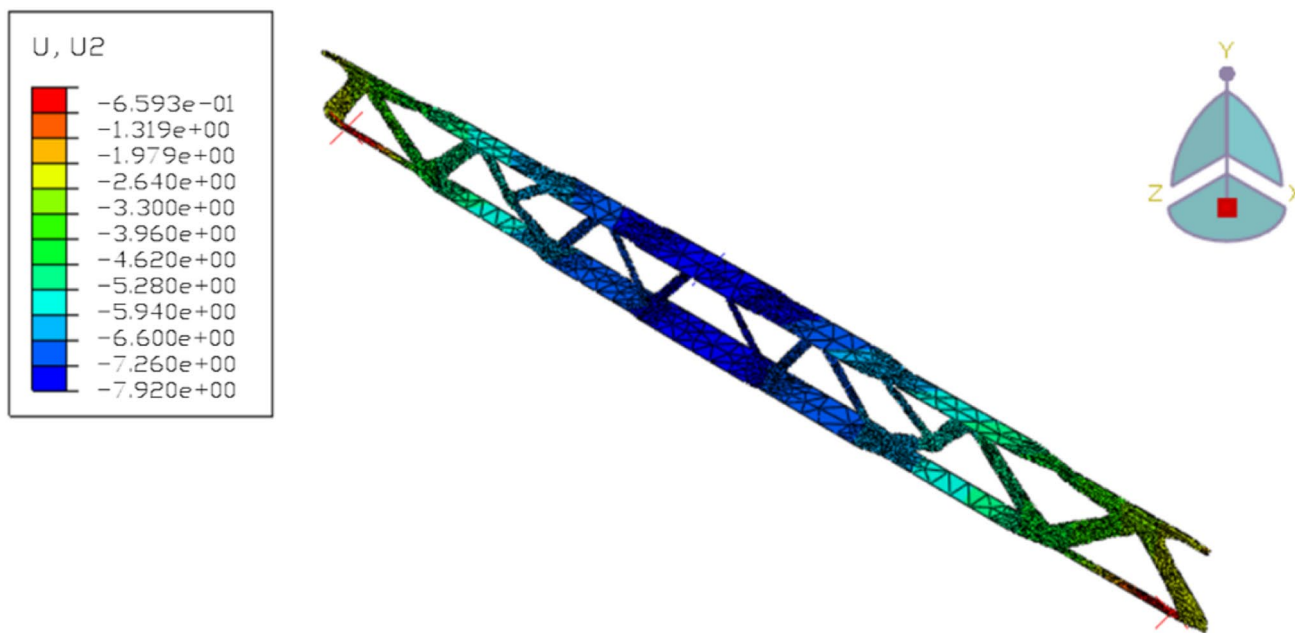

Fig. 9 Engineering vs. true stress–strain curves of WAAM stainless steel

Fig. 10 Results on vertical displacement (in mm)

for some peaks localized next to the plate joints or around abrupt changes in the geometry. The adoption of stress constraints, eventually combined to a full three-dimensional modeling, could remarkably reduce these peaks. Apart from that, it may be noticed that stresses are almost homogenous throughout the flanges. This means that the optimal distribution of flange width is quite effective, assessing that the simplified truss modeling may be a reasonable choice to tackle a preliminary optimization of the I-beam. The web

behaves as a set of trusses. In each one of the web elements, the cross-section is almost uniformly stressed, meaning that most of them act as stiff struts or ties. Only the two extremal elements, due to the width of their cross-section, are acted upon by bending stresses perturbing the aforementioned uniform stress regime.

More detailed studies focused on the local buckling of compressed members should be performed to completely assess
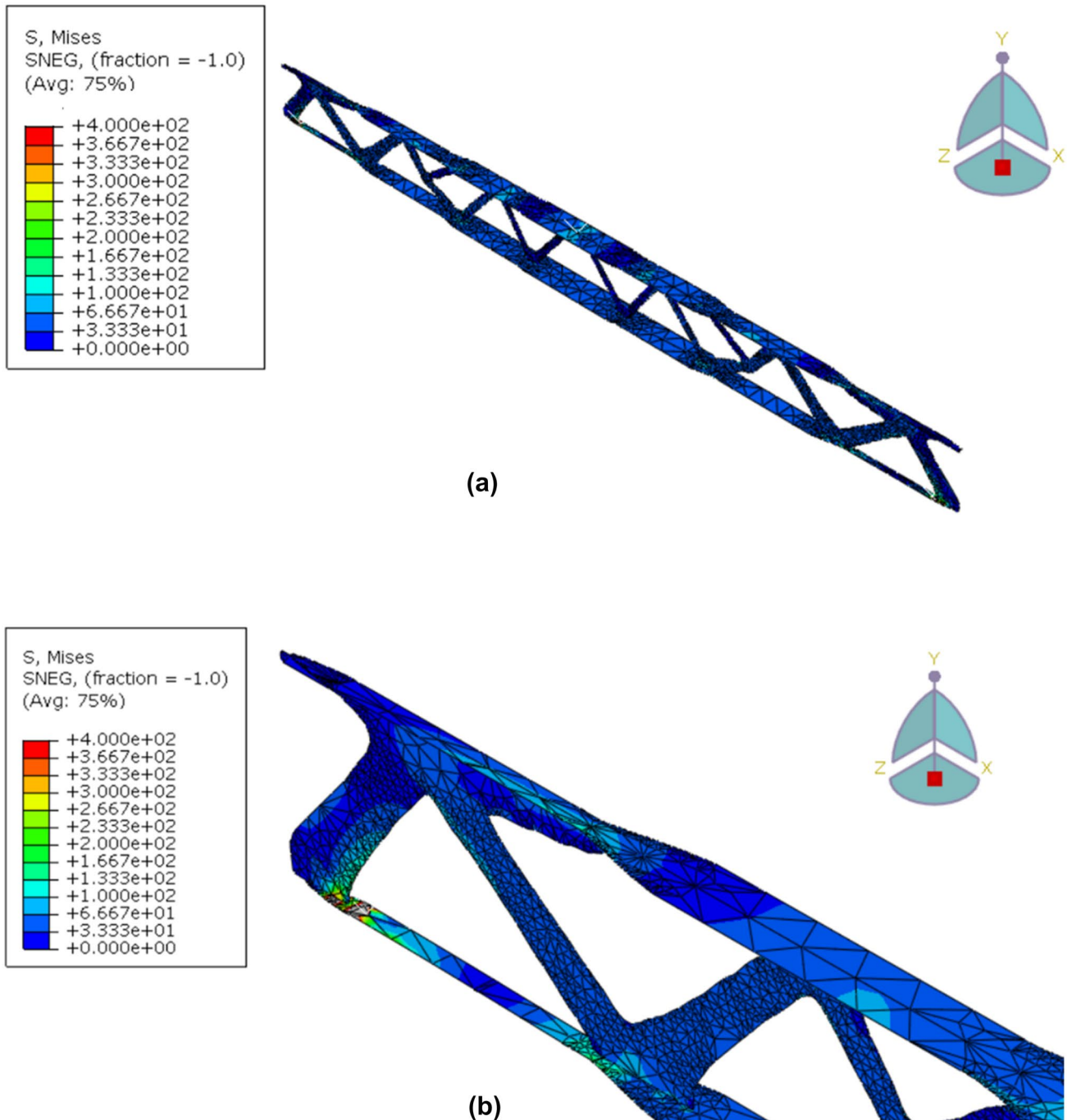

(a)

(b)

Fig. 11 Stress results (in MPa): **a** Von Mises stress map and **b** enlarged view of the beam portion close to one support

the structural performances of the optimized beam, which are, however, out of the scope of the present work.

The results of the numerical simulation may indicate that additional investigations could be performed on the optimized design to further reduce stress concentrations and account for the potential on local buckling of the compressed members. However, these are currently out of the scope of the present work.

6 Conclusions

This paper presents a computational design procedure for the structural design of innovative elements realized with wire-and-arc additive manufacturing (WAAM).

The proposed approach, referred to as "blended" structural optimization, aims at integrating the capabilities of stiffness-based topology optimization procedures with the features and constraints of WAAM technology in an efficient way. The approach combines basic principles of structural design, manufacturing constraints proper of the selected printing process, topology optimization algorithms and numerical simulations to verify the structural performances of the new shapes.

The design approach is applied on the case study of a I-type stainless steel beam on a multi-storey frame building. First, the initial design is set as a 4.5-m long IPE 300 profile with hinge–roller constraints. A stiffness-based topology optimization procedure (specifically tailored for WAAM stainless steel to account for its orthotropic behavior) is then applied. The procedure is set on a maximum allowable deformation equal to $L/250$, according to Eurocodes provisions. The optimization process is run on various combinations of load cases (e.g., permanent and variable loads) typical of the investigated structure. Finally, the structural performances of the optimized design are verified through FE-based numerical simulations. The numerical results on the uniformly distributed load condition confirm the design predictions. More detailed studies are however envisaged in terms of local buckling behavior to assess the global structural behavior of the new element.

The blended structural optimization approach appears to be an efficient way to investigate new effective solutions, with reduced computational time and integrated structural design principles. The method can also pave the way towards an efficient use of WAAM technology to realize innovative structural elements.

Declarations

Conflict of interest The authors declare that they have no known competing financial interests or personal relationships that could have appeared to influence the work reported in this paper.

References

1. Wu P, Wang J, Wang X (2016) A critical review of the use of 3-D printing in the construction industry. Autom Constr 68:21–31
2. Boje C, Guerriero A, Kubicki S, Rezgui Y (2020) Towards a semantic construction digital twin: directions for future research. Autom Constr 114:103179
3. Chadha U, Abrol A, Vora NP, Tiwari A, Shanker SK, Selvaraj SK (2022) Performance evaluation of 3D printing technologies: a review, recent advances, current challenges, and future directions. Prog Addit Manuf. https://doi.org/10.1007/S40964-021-00257-4
4. Sauerwein M, Doubrovski E, Balkenende R, Bakker C (2019) Exploring the potential of additive manufacturing for product design in a circular economy. J Clean Prod 226:1138–1149
5. Priarone PC, Pagone E, Martina F, Catalano AR, Settineri L (2020) Multi-criteria environmental and economic impact assessment of wire arc additive manufacturing. CIRP Ann 69:37–40
6. Buchanan C, Gardner L (2019) Metal 3D printing in construction: a review of methods, research, applications, opportunities and challenges. Eng Struct 180:332–348. https://doi.org/10.1016/j.engstruct.2018.11.045
7. Gardner L, Kyvelou P, Herbert G, Buchanan C (2020) Testing and initial verification of the world's first metal 3D printed bridge. J Constr Steel Res. https://doi.org/10.1016/j.jcsr.2020.106233
8. Lange J, Feucht T, Erven M (2020) 3D printing with steel: Additive Manufacturing for connections and structures. Steel Constr 13:144–153
9. Laghi V, Palermo M, Gasparini G, Trombetti T (2020) Computational design and manufacturing of a half-scaled 3D-printed stainless steel diagrid column. Addit Manuf. https://doi.org/10.1016/j.addma.2020.101505
10. Laghi V, Palermo M, Gasparini G, Girelli VA, Trombetti T (2021) On the influence of the geometrical irregularities in the mechanical response of Wire-and-Arc Additively Manufactured planar elements. J Constr Steel Res 178:106490. https://doi.org/10.1016/j.jcsr.2020.106490
11. Kyvelou P, Slack H, DaskalakiMountanou D, Wadee MA, Ben Britton T, Buchanan C, Gardner L (2020) Mechanical and microstructural testing of wire and arc additively manufactured sheet material. Mater Des 192:108675. https://doi.org/10.1016/j.matdes.2020.108675
12. Laghi V, Tonelli L, Palermo M, Bruggi M, Sola R, Ceschini L, Trombetti T (2021) Experimentally-validated orthotropic elastic model for Wire-and-Arc Additively Manufactured stainless steel. Addit Manuf 42:101999. https://doi.org/10.1016/j.addma.2021.101999
13. Laghi V, Palermo M, Tonelli L, Gasparini G, Ceschini L, Trombetti T (2020) Tensile properties and microstructural features of 304L austenitic stainless steel produced by wire-and-arc additive manufacturing. Int J Adv Manuf Technol. https://doi.org/10.1007/s00170-019-04868-8

14. Dinovitzer M, Chen X, Laliberte J, Huang X, Frei H (2019) Effect of wire and arc additive manufacturing (WAAM) process parameters on bead geometry and microstructure. Addit Manuf 26:138–146. https://doi.org/10.1016/j.addma.2018.12.013

15. Ye J, Kyvelou P, Gilardi F, Lu H, Gilbert M, Gardner L (2021) An end-to-end framework for the additive manufacture of optimized tubular structures. IEEE Access 9:165476–165489

16. Christensen PW, Klarbring A (2008) An introduction to structural optimization. Springer Science & Business Media

17. Bendsøe M, Sigmund O (2003) Topology optimization—theory, methods and applications. Springer EUA, New York

18. Rong Y, Zhao Z-L, Feng X-Q, Xie YM (2022) Structural topology optimization with an adaptive design domain. Comput Methods Appl Mech Eng 389:114382

19. Saadlaoui Y, Milan JL, Rossi JM, Chabrand P (2017) Topology optimization and additive manufacturing: comparison of conception methods using industrial codes. J Manuf Syst. https://doi.org/10.1016/j.jmsy.2017.03.006

20. Li S, Yuan S, Zhu J, Wang C, Li J, Zhang W (2020) Additive manufacturing-driven design optimization: building direction and structural topology. Addit Manuf 36:101406. https://doi.org/10.1016/j.addma.2020.101406

21. Tonelli L, Sola R, Laghi V, Palermo M, Trombetti T, Ceschini L, Ceschini PL, Trombetti PT, Tomaso Trombetti P (2021) Influence of inter-layer forced air cooling on microstructure and mechanical properties of Wire Arc Additively Manufactured 304L austenitic stainless steel. Steel Res Int. https://doi.org/10.1002/srin.202100175

22. Kyvelou P, Slack H, Mountanou DD, Wadee MA, Ben Britton T, Buchanan C, Gardner L (2020) Mechanical and microstructural testing of wire and arc additively manufactured sheet material. Mater Des. https://doi.org/10.1016/J.MATDES.2020.108675

23. Laghi V, Palermo M, Tonelli L, Gasparini G, Girelli VA, Ceschini L, Trombetti T (2022) Mechanical response of dot-by-dot wire-and-arc additively manufactured 304L stainless steel bars under tensile loading. Constr Build Mater 318:125925

24. Silvestru V-A, Ariza I, Vienne J, Michel L, Aguilar Sanchez AM, Angst U, Rust R, Gramazio F, Kohler M, Taras A (2021) Performance under tensile loading of point-by-point wire and arc additively manufactured steel bars for structural components. Mater Des 205:109740. https://doi.org/10.1016/j.matdes.2021.109740

25. Kanyilmaz A, Demir AG, Chierici M, Berto F, Gardner L, Kandukuri SY, Kassabian P, Kinoshita T, Laurenti A, Paoletti I, du Plessis A, Razavi SMJ (2022) Role of metal 3D printing to increase quality and resource-efficiency in the construction sector. Addit Manuf 50:102541. https://doi.org/10.1016/J.ADDMA.2021.102541

26. Gardner L, Kyvelou P, Buchanan C (2019) Testing of wire and arc additively manufactured tubular sections. p 978–981. https://doi.org/10.3850/978-981-11-0745-0

27. Ji L, Lu J, Liu C, Jing C, Fan H, Ma S (2017) Microstructure and mechanical properties of 304L steel fabricated by arc additive manufacturing. MATEC Web Conf. https://doi.org/10.1051/matecconf/201712803006

28. Haden CV, Zeng G, Carter FM, Ruhl C, Krick BA, Harlow DG (2017) Wire and arc additive manufactured steel: tensile and wear properties. Addit Manuf 16:115–123. https://doi.org/10.1016/j.addma.2017.05.010

29. Gordon JV, Haden CV, Nied HF, Vinci RP, Harlow DG (2018) Fatigue crack growth anisotropy, texture and residual stress in austenitic steel made by wire and arc additive manufacturing. Mater Sci Eng A 724:431–438. https://doi.org/10.1016/j.msea.2018.03.075

30. Ge J, Lin J, Chen Y, Lei Y, Fu H (2018) Characterization of wire arc additive manufacturing 2Cr13 part: process stability, microstructural evolution, and tensile properties. J Alloys Compd 748:911–921. https://doi.org/10.1016/j.jallcom.2018.03.222

31. Yilmaz O, Ugla AA (2017) Microstructure characterization of SS308LSi components manufactured by GTAW-based additive manufacturing: shaped metal deposition using pulsed current arc. Int J Adv Manuf Technol 89:13–25. https://doi.org/10.1007/s00170-016-9053-y

32. Hadjipantelis N, Weber B, Gardner L (2021) Characterisation of the anisotropic response of wire and arc additively manufactured stainless steel. Ce/Papers 4:1757–1766

33. Steels M (2004) Metallography and microstructures of stainless steels maraging steels. ASM Handb V9(9):1–27. https://doi.org/10.1361/asmhba0003767

34. European Committee for Standardization (CEN) (2002) EN 1990: Eurocode 0—basis of structural design

35. Holicky M (2009) Reliability analysis for structural design. SUN press

36. ISO 2394 (1998) General principles on reliability for structures

37. Laghi V, Palermo M, Gasparini G, Veljkovic M, Trombetti T (2020) Assessment of design mechanical parameters and partial safety factors for Wire-and-Arc Additive Manufactured stainless steel. Eng Struct 225:111314. https://doi.org/10.1016/j.engstruct.2020.111314

38. Okita T, Kawabata T, Murayama H, Nishino N, Aichi M (2019) A new concept of digital twin of artifact systems: synthesizing monitoring/inspections, physical/numerical models, and social system models. Procedia CIRP 79:667–672. https://doi.org/10.1016/j.procir.2019.02.048

39. Cascone F, Faiella D, Tomei V, Mele E (2021) A structural grammar approach for the generative design of diagrid-like structures. Building. https://doi.org/10.3390/buildings11030090

40. Wang H, Du W, Zhao Y, Wang Y, Hao R, Yang M (2021) Joints for treelike column structures based on generative design and additive manufacturing. J Constr Steel Res 184:106794. https://doi.org/10.1016/J.JCSR.2021.106794

41. Wang W, Munro D, Wang CCL, van Keulen F, Wu J (2020) Space-time topology optimization for additive manufacturing. Struct Multidiscip Optim 61:1–18

42. Kanyilmaz A, Berto F (2019) Robustness-oriented topology optimization for steel tubular joints mimicking bamboo structures. Mater Des Process Commun 1:e43

43. Bruggi M, Laghi V, Trombetti T (2021) Simultaneous design of the topology and the build orientation of Wire-and-Arc Additively Manufactured structural elements. Comput Struct. https://doi.org/10.1016/j.compstruc.2020.106370

44. Bruggi M, Laghi V, Trombetti T (2022) Optimal design of Wire-and-Arc Additively Manufactured I-beams for prescribed deflection. Comput Assist Methods Eng Sci

45. LayOpt, (n.d.). https://www.layopt.com/truss/

46. European Committee for Standardization (CEN) (2015) EN 1993 1–4: Eurocode 3—Design of steel structures, part 1–4: General rules, supplementary rules for stainless steel

47. Dassault Systemes (2016) Abaqus CAE

48. Ramberg W, Osgood WR (1943) Description of stress-strain curves by three parameters

49. Rasmussen KJR (2001) Full-range stress–strain curves for stainless steel alloys. Res Rep Univ Sydney Dept Civ Eng 59:1–44